ISSN 1674-1056
http://cpb.iphy.ac.cn
http://iopscience.iop.org/cpb
中国物理 B
Chinese Physics
中国物理
Chinese Physics B

Investigation on the drives of the poloidal flow in the ohmic and biased electrode experiments

Yi Yu(余羿), Tao Lan(兰涛), Min Xu(许敏), Yizhi Wen(闻一之)

Citation: Chin. Phys. B . 2019, 28(3): 035202. **doi:** 10.1088/1674-1056/28/3/035202
Journal homepage: http://cpb.iphy.ac.cn; http://iopscience.iop.org/cpb

What follows is a list of articles you may be interested in

Fast parallel Grad-Shafranov solver for real-time equilibrium reconstruction in EAST tokamak using graphic processing unit

Yao Huang(黄耀), Bing-Jia Xiao(肖炳甲), Zheng-Ping Luo(罗正平)
Chin. Phys. B . 2017, 26(8): 085204. **doi:** 10.1088/1674-1056/26/8/085204

Comparison benchmark between tokamak simulation code and TokSys for Chinese Fusion Engineering Test Reactor vertical displacement control design

Qing-Lai Qiu(仇庆来), Bing-Jia Xiao(肖炳甲), Yong Guo(郭勇), Lei Liu(刘磊), Yue-Hang Wang(汪悦航)
Chin. Phys. B . 2017, 26(6): 065205. **doi:** 10.1088/1674-1056/26/6/065205

A divertor plasma configuration design method for tokamaks

Yong Guo(郭勇), Bing-Jia Xiao(肖炳甲), Lei Liu(刘磊), Fei Yang(杨飞), Yuehang Wang(汪悦航), Qinglai Qiu(仇庆来)
Chin. Phys. B . 2016, 25(11): 115201. **doi:** 10.1088/1674-1056/25/11/115201

Effects of *q*-profiles of a weak magnetic shear on energetic ion excited *q*=1 mode in tokamak plasmas

Ze-Yu Li(李泽宇), Xian-Qu Wang(王先驱), Xiao-Gang Wang(王晓钢)
Chin. Phys. B . 2016, 25(1): 015203. **doi:** 10.1088/1674-1056/25/1/015203

Start-up phase plasma discharge design of a tokamak via control parameterization method

Guo Shan, Xu Ke, Xu Chao, Ren Zhi-Gang, Xiao Bing-Jia
Chin. Phys. B . 2015, 24(3): 035202. **doi:** 10.1088/1674-1056/24/3/035202

Investigation on the drives of the poloidal flow in the ohmic and biased electrode experiments*

Yi Yu(余羿)[1,2,†], Tao Lan(兰涛)[1], Min Xu(许敏)[3], and Yizhi Wen(闻一之)[1]

[1] *University of Science and Technology of China, Hefei* 230026, *China*
[2] *School of Science, Xihua University, Chengdu* 610041, *China*
[3] *Southwestern Institute of Physics, Chengdu* 610041, *China*

(Received 31 October 2018; revised manuscript received 14 December 2018; published online 23 January 2019)

The experimental investigation on the drives of the poloidal flow in KT-5D tokamak are presented. It is found that the poloidal flow is the main contributor to the radial electric field, and the Reynolds stress can drive significant poloidal flows in ohmic discharges. The investigation on the relationship between the radial gradient of Reynolds stress and the poloidal flow in biasing discharges indicates that not only Reynolds stress but also the Lorentz's force can drive the poloidal flow.

Keywords: radial electric field, poloidal flow, Reynolds stress

PACS: 52.55.Fa, 52.25.Gj, 52.35.Ra **DOI:** 10.1088/1674-1056/28/3/035202

1. Introduction

Sheared poloidal flow is believed to be one of the most effective measures in suppressing turbulence and the corresponding anomalous transport in magnetically confined fusion plasmas. With a sufficiently strong gradient in the direction which is perpendicular to the propagating direction of the flow, the shear flow will distort the turbulent eddies and finally tear them apart into smaller ones. As a result, the radial correlation length of the turbulence should be reduced. This will lead to an enhancement of the energy dissipation of the turbulence, if the intensity of the turbulence does not change. The gradients of the density and the temperature, which are the free energy source of the drift-wave turbulence, will not be changed by the shear flow. As a result, the balance of the drift-wave turbulence will be broken once the shear flow is excited. The new balance will shape in smaller turbulence intensity. The reductions of the turbulence intensity and the characteristic length of the eddies will reduce the diffusion coefficient. From this point of view, the poloidal flows will restrain the anomalous transport.

Many related investigations have been carried out because of the importance of the sheared poloidal flow in plasma confinement.[1–4] The ion orbit loss caused by the interaction with the limiter was used to explain the generation of sheared poloidal flows.[5–7] The Reynolds stress of turbulence may drive significant poloidal flows in the plasma boundary region.[8–10] Poloidal flow, together with the Reynolds stress, may play important roles in the L–H mode transition. Experiments in the axially symmetric diverter experiment (ASDEX) tokamak showed the increase of the poloidal flow and the pressure gradient in the L–H transition.[11] The poloidal flow is the main contributor to the radial electric field $\boldsymbol{E}_r$ at the beginning of the H-mode,[12] and it is also the main contributor to $\boldsymbol{E}_r$ in the transport barrier.[13] Experiments in DIII-D tokamak demonstrated that the threshold power of L–H transition decreases as the edge toroidal rotation decreases, and at a low edge toroidal rotation level, large changes in the shear of the poloidal velocity of the edge turbulent eddies have been observed prior to the L–H transition which may be strong enough to induce the transition.[14] Biasing provides an effective way to conveniently control $\boldsymbol{E}_r$ and shear. The biasing H-mode experiments have a long history starting from the experiment in tokamak for technology oriented research (TEXTOR), followed by a well organized quantification of the role of Reynolds stress on the transition.[15,16] In the biasing experiments, radial current drives poloidal flow, and then this poloidal flow drives $\boldsymbol{E}_r$,[17] resulting in the reduction of fluctuations not only in tokamak plasma[18] but also in reversed field pinch[19] and linear plasmas.[20] The probe data in tokamaks have revealed that the Reynolds stress component shows a radial gradient close to the velocity shear layer location, implying that Reynolds stress may drive significant poloidal flows in the plasma boundary region.[21] A detailed overview of biasing experiments to understand the mechanism of poloidal flow drives and fluctuation reduction in TEXTOR, Czech Academy of Sciences torus (CASTOR), T10, and Instituto Superior Técnico tokamak (ISTTOK) and in reversed-field experiment (RFX) reversed field pinch can be found in Ref. [22].

In experiments, there are few studies on the Reynolds stress parameter scaling and correlation with poloidal flows.

*Project supported by the National Natural Science Foundation of China (Grant No. 11875124), the National Magnetic Confinement Fusion Energy Research Project, China (Grant No. 2015GB120002), and the National Key Research and Development Program of China (Grant No. 2017YFE0300405).

†Corresponding author. E-mail: yuyi@ustc.edu.cn

© 2019 Chinese Physical Society and IOP Publishing Ltd

This partly comes from the difficulty of diagnosing the Reynolds stress and some other main parameters in the high-temperature large tokamaks. More research is needed to quantify its relative importance as compared with other mechanisms. In this article, studies on the drives of the poloidal flow in biasing experiments are presented. The rest of this article is arranged as follows. In Section 2, a brief introduction of KT-5D device is presented, together with the setting of the biased dual-electrode. The main experimental results and discussion are put in Section 3, and Section 4 is a brief conclusion.

2. Experiment setup

The experiments are conducted in the double functional device KT-5D.[23,24] In the pulse mode discharge, KT-5D is an ohmically heated small tokamak with a major radius of $R = 32.5$ cm, a minor radius of $a = 12.5$ cm, and a limiter radius of 9 cm. The coils can provide a toroidal field of up to 7000 Gauss with a maximal flattop time period of 8 ms. The plasma current is 16 KA. The electron temperature is about 100 eV and the plasma density is of the order of 10^{19} m^{-3}. These discharging parameters are much lower compared with large tokamaks, while they make KT-5D a convenient device for some fundamental physical studies, for example, the biasing experiments performed in this article. There are two main advantages for this pure simple ohmic discharge. One is the stable working condition of KT-5D which is mainly determined by the stable capacitor banks, without any complicated components such as wave heating and neutral beam injection. This characteristic results in a high repeatability of KT-5D discharging. Keeping the same discharging parameters, such as the magnetic field and working gas pressure, we can accumulate data from many shots. The other advantage is that the flattop time is so short that Langmuir probes can work in plasma without being burned.

Biased dual-electrode is used in experiments to change the radial electric field and to improve the confinement. Two electrodes, which are made of stainless steel discs with a diameter of 2 cm and a thickness of 0.4 cm, are located at the radial locations of $r = 3$ cm and $r = 7$ cm in the same poloidal cross section, as shown in Fig. 1. The biasing voltages are supplied from two charged capacitor banks (22 mF), controlled by the thyristor switches.

Two biasing voltage combinations are set to these two electrodes in the experiments. One is called shot I_N, which means that a negative voltage of about -200 V is loaded on the inner electrode and no biasing voltage is loaded on the outer one. Similarly, the other is called shot I_N_O_P, which is the acronym for inner electrode, negative 200 V, outer electrode, and positive 200 V. Experiments without biasing are marked as NB (i.e., no biasing) in this article.

Langmuir probe[25,26] arrays work as the main diagnosing tool in these experiments. A tungsten filament with a diameter of 0.5 mm is chosen as the probe tip. It can move radially from $r = 5$ cm to 10 cm in the low field side. The measurement in a radial location of $r < 5$ cm is not compelling for the reason that the probe tips are sometimes overheated because of the high core plasma parameters. In the experiments presented in this article, the probe tips stay in a fixed radial location without moving in each shot. The signals in another location are diagnosed in another shot. The tip location is adjusted artificially between shots. This manner is very different to that in large tokamaks in which edge probes are pneumatically movable and scan plasma in a designed radial range. The correctness is based on the high repeatability of KT-5D discharging as has been mentioned above. The moving step length between adjacent diagnosing locations is 2.5 mm. The temporal resolution of the probes is 1 μs.

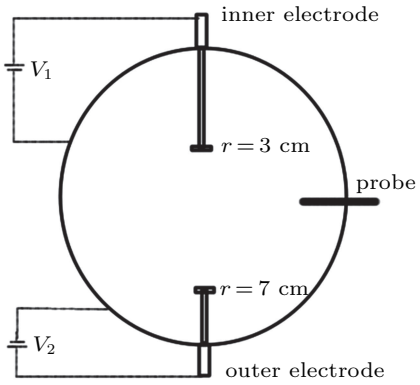


Fig. 1. Setting of the two biasing electrodes.

3. Results and discussion

Figures 2(a)–2(f) respectively show the time revolutions of the positive biasing voltage of outer electrode V_2, the current I_2 led by the outer electrode, the negative biasing voltage of inner electrode V_1, the current I_1 led by the inner electrode, the floating potential of plasma V_f, and the radial electric field $\boldsymbol{E}_r$ diagnosed by Langmuir probes at a radial location of $r = 7.5$ cm in shot I_N_O_P. The poloidal flow is determined by $\boldsymbol{E}_r \times \boldsymbol{B}$ flow, which has the same time revolution as $\boldsymbol{E}_r$ because of the constant $B \propto 1/(32.5\ \text{cm} + r)$ at a fixed location r. Biasing voltage is loaded at the time point of about 1.17 ms.

The components of the radial electric field $\boldsymbol{E}_r$ are widely studied. The radial force equilibrium equation is used to analyze $\boldsymbol{E}_r$[15,27]

$$\boldsymbol{E}_r = \frac{1}{n_i Z_i e}\nabla P_i - \boldsymbol{u}_{\theta i}\boldsymbol{B}_\phi + u_\phi \boldsymbol{B}_\theta, \tag{1}$$

where Z_i, e, n_i, and P_i are the charge number of ion, the electron charge, the density of ions, and the pressure of ions, respectively. The subscripts of θ and φ denote the poloidal and

toroidal components. The experimentally measured profiles of $\boldsymbol{E}_r$ as a function of radius r are shown in Fig. 3. Although there is a pronounced $\boldsymbol{E}_r$ well around the radial position of $r \sim 8.5$ cm, biasing or no biasing, biasing does change the profile and deepen the well of $\boldsymbol{E}_r$.

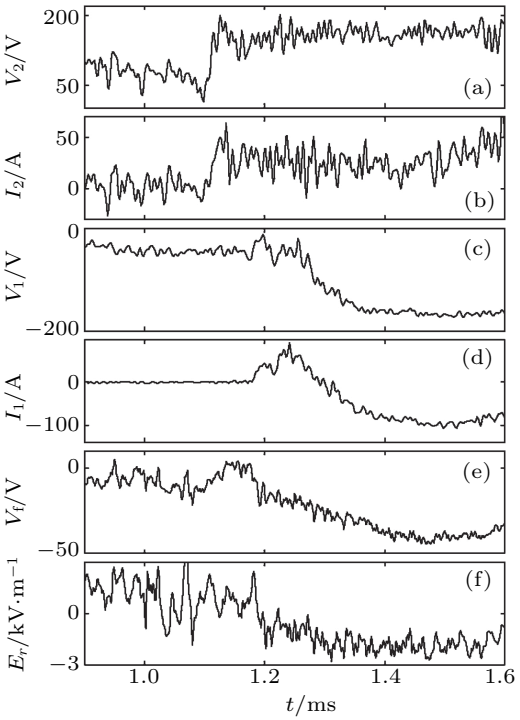


Fig. 2. Time revolutions of main discharging and plasma parameters in shot I_N_O_P at a radial location of $r = 7.5$ cm: (a) the positive biasing voltage of outer electrode V_2, (b) the current I_2 led by the outer electrode, (c) the negative biasing voltage of inner electrode V_1, (d) the current I_1 led by the inner electrode, (e) the floating potential of plasma V_f, and (f) the radial electric field E_r.

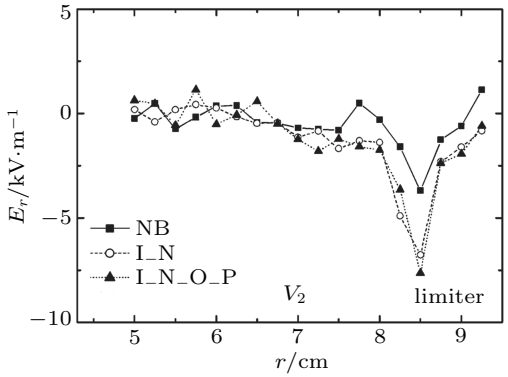


Fig. 3. The profiles of the radial electric field as a function of radius r.

In the KT-5D tokamak discharges, the toroidal flow term and the pressure gradient term are almost equal and opposite in this case, which has a similar discharging configuration as that in Ref. [28]. These two terms to a large degree are canceled out in the experiments. It is therefore not difficult to draw the conclusion that the poloidal flow term is predominant for $\boldsymbol{E}_r$.

The measured profiles of the poloidal flow are shown in Fig. 4 as a function of radius r. Every profile peaks at the radial position of $r \sim 8.5$ cm, and as expected, biasing increases the peak. The wells in Fig. 3 and peaks in Fig. 4 are located at the same radial position ($r \sim 8.5$ cm) and biasing takes effect simultaneously on $\boldsymbol{E}_r$ and poloidal flow, showing the fact that poloidal flow dominates $\boldsymbol{E}_r$, which has already been drawn in the preceding paragraph.

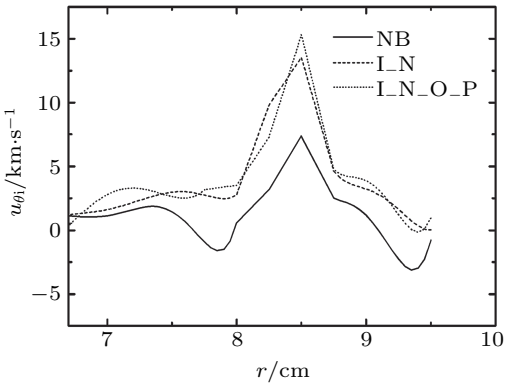


Fig. 4. The distribution of the poloidal flow as a function of radius r.

It should be noted that in Figs. 3 or 4, the plasma behavior in I_N_O_P shot shows similarity with that in I_N shot. More experimental evidence can be found in Fig. 2. In these figures, one can clearly see that the voltage V_2 and current I_2 of the outer electrode change quickly when the biasing voltage is applied, while V_1 and I_1 of the inner electrode change much more slowly. The floating potential V_f and the radial electric field $\boldsymbol{E}_r$ (/poloidal $\boldsymbol{E}_r \times \boldsymbol{B}$ flow) follow similar evolutions as V_1 and I_1, which indicates the dominate role of the inner negative electrode. Similar conclusion can also be drawn in some of the following figures. The difference between these two shot modes and the underlying mechanism are out of the scope of this article and are detailed elsewhere.[29] Therefore, in this article, these two kinds of biasing modes can almost be considered as the same one.

In the case with no biasing, which means no zero-order component of radial current, the poloidal momentum balance equation is given by[30]

$$\frac{\partial \langle \boldsymbol{u}_{\theta i} \rangle}{\partial t} = -\frac{\partial}{\partial r} \langle \tilde{\boldsymbol{u}}_{ri} \tilde{\boldsymbol{u}}_{\theta i} \rangle - \mu_\theta \langle \boldsymbol{u}_{\theta i} \rangle, \tag{2}$$

where $\tilde{\boldsymbol{u}}_{ri}, \tilde{\boldsymbol{u}}_{\theta i}$ stand for the radial and poloidal velocity fluctuation of plasmas, the correlation coupling of these velocity fluctuations $\langle \tilde{\boldsymbol{u}}_{ri} \tilde{\boldsymbol{u}}_{\theta i} \rangle$ stands for the Reynolds stress tensor, $\langle\ \rangle$ stands for flux surface average, and μ_i stands for neoclassical viscous coefficient. In the poloidal direction, neoclassical viscous is balanced against the radial gradient of Reynolds stress. $\tilde{\boldsymbol{u}}_{ri}, \tilde{\boldsymbol{u}}_{\theta i}$ can be calculated from the fluctuations of poloidal and radial electric fields

$$\tilde{\boldsymbol{u}}_{ri} = \frac{\tilde{\boldsymbol{E}}_\theta}{\boldsymbol{B}_\phi} = -\frac{1}{\boldsymbol{B}_\phi} \frac{\partial \tilde{\varphi}}{r \partial \theta}, \quad \tilde{\boldsymbol{u}}_{\theta i} = -\frac{\tilde{\boldsymbol{E}}_r}{\boldsymbol{B}_\phi} = \frac{1}{\boldsymbol{B}_\phi} \frac{\partial \tilde{\varphi}}{\partial r}. \tag{3}$$

The radial distributions of Reynolds stress R_s in KT-5D discharges with and without biasing are shown in Fig. 5. From

this figure, one can clearly see the peak shift of Reynolds stress caused by biasing. In the discharge with no biasing, the positions where the Reynolds stress gradient is the biggest are just the velocity shear layer of the poloidal flow. This means that the Reynolds stress may drive significant poloidal flows. From the viewpoint of momentum balance, we can draw the conclusion that the momentum transfers from the turbulence into poloidal shear flow via Reynolds stress.

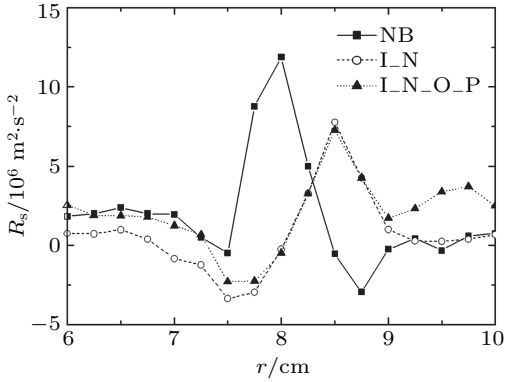


Fig. 5. The radial distributions of Reynolds stress in the discharges with and without biasing.

Here, we use Stix neoclassical viscous term instead of $\mu_\theta\langle \boldsymbol{u}_{\theta i}\rangle$

$$\mu_\theta\langle \boldsymbol{u}_{\theta i}\rangle = \left(\frac{\sqrt{\pi}}{2}\frac{qV_{th}}{R}\exp(-U_{pm}^2)+\frac{1}{2}\frac{\upsilon_{ii}q^2}{1+U_{pm}^2}\right) \times(\langle \boldsymbol{u}_{\theta i}\rangle - V_\theta^{Neo}), \quad (4)$$

where $U_{pm}=-E_r/B_\theta V_{th}$, $\upsilon_{ii}=n_i T_i^{-3/2}/2\times 10^{12}$ is the collision frequency of ions, $V_{th}=(2T_i/m_i)^{1/2}$ is the hot velocity of ions, $q=rB_{\phi 0}/RB_\theta(r)$ is the safety factor, and $V_\theta^{Neo}=(-0.5/eB_{\phi 0})(\mathrm{d}T_i/\mathrm{d}r)$ is the neoclassical velocity. The comparison between the neoclassical viscous term $\mu_\theta\langle \boldsymbol{u}_{\theta i}\rangle$ and the radial gradient of Reynolds stress $-\partial\langle \tilde{\boldsymbol{u}}_{ri}\tilde{\boldsymbol{u}}_{\theta i}\rangle/\partial r$ is drawn in Fig. 6. In general, the profiles of these two terms show similar trends and are in accord with each other at most of radial locations. It is now clear that in the ohmic discharge, the Reynolds stress of turbulence is the main drive of poloidal flows, and that it is also an important cause of the radial electric field.

In the discharges with biasing, the Reynolds stress and its radial gradient decrease (see Fig. 5), but at the same time, the poloidal flow increases (see Fig. 4) compared with those in the discharges with no biasing. This means that the Reynolds stress is not the only drive of poloidal flow in this case. Lorentz's force caused by the radial currents is another drive. The theory of L–H transition by biasing believes the balance between the neoclassical viscous term $\mu_\theta\langle \boldsymbol{u}_{\theta i}\rangle$ and the poloidal Lorentz's force $\boldsymbol{J}\times\boldsymbol{B}$ which is caused by the radial currents

$$\boldsymbol{J}_r\times\boldsymbol{B}=\nabla\cdot\prod\equiv n_i m_i\mu_\theta \boldsymbol{u}_{\theta i}. \quad (5)$$

Here, $\boldsymbol{J}_r$ includes two parts, namely, the radial electric current introduced by the biased electrode and the equivalent radial electric current caused by the Reynolds stress of fluctuation of the poloidal flow. Π is the Maxwell stress tensor. Viscous coefficient μ_θ remains nearly constant in the case of low flow velocity. It reaches a maximum value when the normalized ion–ion collision ratio ν_{*i} reaches its bifurcation threshold value of 1.5, and decreases rapidly once ν_{*i} exceeds this threshold.[5] The sharp falling of μ_θ will bring a bigger flow velocity and the decrease of the electric current. For KT-5D plasma investigated in this article, a roughly estimated ν_{*i} is 0.092, which is far from this threshold value of 1.5. So we approximately consider μ_θ as a slowly changing value in different flow velocities. $\boldsymbol{J}_r\times\boldsymbol{B}$ force provides an additional poloidal flow as shown in Eq. (5). Comparing with NB experiment, in biasing experiments, the poloidal flow (peaking at $r=8.5$ cm, Fig. 4) almost doubles (from about 5 km/s to about 13 km/s), while the Reynolds stress gradient is negatively reduced by half (from about -14 to about 7, Fig. 5). This indicates that the Reynolds stress only accounts for a small part of the contribution to the poloidal flow in biasing experiments, while Lorentz's force caused by the radial currents dominates.

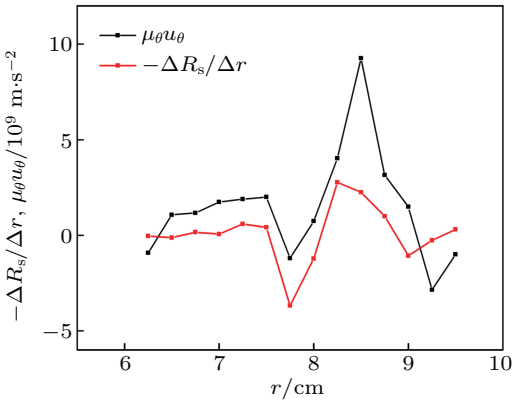


Fig. 6. The comparison between the neoclassical viscous term and the radial gradient of Reynolds stress. It should be noted that the y-coordinate is negative radial gradient of Reynolds stress.

4. Conclusion

Dual-electrode biasing experiments are performed in KT-5D tokamak to investigate the drives of the poloidal flow. The poloidal flow is experimentally confirmed to be the main contributor to $\boldsymbol{E}_r$. In the discharges with no biasing, the positions where the Reynolds stress gradient is the biggest are just the velocity shear layer of the poloidal flow. This implies that the Reynolds stress may drive significant poloidal flows. In the biasing electrode experiments, both the Reynolds stress and the radial gradient of it decrease, while the poloidal flow increases. This means that not only the Reynolds stress but also the Lorentz's force caused by the radial currents can drive the poloidal flow. Lorentz's force dominates the poloidal flow in biasing experiments.

References

[1] Ritz C P, Lin H, Rhodes T L and Wootton A J 1990 *Phys. Rev. Lett.* **65** 2543

[2] Rempel T P, Spragins C W, Prager S C, Assadi S, Hartog Den D J and Hokin S 1991 *Phys. Rev. Lett.* **67** 1438

[3] Endler M, Niedermeyer H, Giannone L, Holzhauer E, Rudyj A, Theimer G and Tsois N 1995 *Nucl. Fusion* **35** 1307

[4] Chapman B E, Chiang C S, Prager S C, Sarff J S and Stoneking M R 1998 *Phys. Rev. Lett.* **80** 2137

[5] Shaing K C and Grume E C 1989 *Phys. Rev. Lett.* **63** 2369

[6] Itoh K and Itoh S 1996 *Plasma Phys. Control. Fusion* **38** 1

[7] Kobayashi T, Itoh K, Ido T, Kamiya K, Itoh S I, Miura Y, Nagashima Y, Fujisawa A, Inagaki S, Ida K and Hoshino K 2016 *Plasmas. Sci. Rep.* **6** 30720

[8] Diamond P H and Kim Y B 1991 *Phys. Fluids B* **3** 1626

[9] Carreras B A, Lynch V E and Garcia L 1991 *Phys. Fluids B* **3** 1438

[10] Garcia L, Carreras B A, Lynch V E and Diamond P H 1992 *Proceedings of the* 14*th Conference on Plasma Physics and Controlled Nuclear Fusion Research*, September 30–October 7, 1992 Würzburg, Germany, vol. 2, p. 225

[11] Burrel K H 1994 *Plasma Phys. Control. Fusion* **36** A291

[12] Moyer R A, Burrell K H, Carlstrom T N, Coda S, Conn R W, Doyle E J, Gohil P, Groebner R J, Kim J, Lehmer R, Peebles W A, Porkolab M, Rettig C L, Rhodes T L, Seraydarian T P, Stockdale T, Thomas D M, Tynan G R and Watkins J G 1995 *Phys. Plasmas* **2** 2397

[13] LeBlanc B, Batha S, Bell R, *et al.* 1995 *Phys. Plasmas* **2** 741

[14] Gohil P, McKee G R, Schlossberg D, Schmitz L and Wang G 2008 *J. Phys.: Conf. Ser.* **123** 012017

[15] Weynants R R and Taylor R J 1990 *Nucl. Fusion* **30** 945

[16] Shesterikov I, Xu Y, Tynan G R, Diamond P H, Jachmich S, Dumortier P, Vergote M, Van Schoor M, Van Oost G and TEXTOR Team 2013 *Phys. Rev. Lett.* **111** 055006

[17] Cornelis J, Sporken R, Van Oost G and Weynants R R 1994 *Nucl. Fusion* **34** 171

[18] Nascimento I C, Kuznetsov Y K, Severo J H F, Fonseca A M M, Elfimov A, Bellintani V, Machida M, Heller M V A P, Galvao R M O, Sanada E K and Elizondo J I 2005 *Nucl. Fusion* **45** 796

[19] Craig D, Almagri A F, Anderson J K, Chapman J T, Chiang C S, Crocker N A, Hartog Den D J, Fiksel G, Prager S C, Sarff J S and Stoneking M R 1997 *Phys. Rev. Lett.* **79** 1865

[20] Shinohara S, Matsuoka N and Yoshinaka T 1999 *Jpn. J. Appl. Phys.* **38** 4321

[21] Hidalgo C, Silva C, Pedrosa M A, Sanchez E, Fernandes H and Varandas C A F 1999 *Phys. Rev. Lett.* **83** 2203

[22] Oost Van G, Adamek J, Antoni V, *et al.* 2003 *Plasma Phys. Control. Fusion* **45** 621

[23] Yu Y, Wang Z, Xu M, Zhu Z, Lu R, Wen Y, Yu C, Wan S, Liu W, Wang J, Xu X and Hu L 2006 *Rev. Sci. Instr.* **77** 123502

[24] Yu Y, Wen Y, Yu C, Wan S and Liu W 2008 *Rev. Sci. Instr.* **79** 083507

[25] Chen S L and Sekiguchi T 1965 *J. Appl. Phys.* **36** 2363

[26] Hutchinson I H 2014 *Principles of Plasma Diagnostics* (2nd edn.) (Cambridge: Cambridge University Press) p. 60

[27] Groebner R J, Burrell K H and Seraydarian R P 1990 *Phys. Rev. Lett.* **64** 3015

[28] Wang C, Pan G, Yu C, Wen Y, Wan S, Wang Z, Liu W, Sun X, Wang J and Gao H 2002 *IEEE Trans. Plasma Sci.* **30** 625

[29] Yu Y, Lu R, Wang C, Pan G, Wen Y, Yu C, Ma J, Wan S and Liu W 2006 *Plasma Sci. Tech.* **8** 91

[30] Tala T, Andrew Y, Crombe K, *et al.* 2007 *Nucl. Fusion* **47** 1012